Neuron, Vol. 32, 711–721, November 20, 2001, Copyright ©2001 by Cell Press

Cellular Basis for the Response to Second-Order Motion Cues in Y Retinal Ganglion Cells

Jonathan B. Demb,[1] Kareem Zaghloul, and Peter Sterling
Department of Neuroscience
University of Pennsylvania School of Medicine
Philadelphia, Pennsylvania 19104

Summary

We perceive motion when presented with spatiotemporal changes in contrast (second-order cue). This requires linear signals to be rectified and then summed in temporal order to compute direction. Although both operations have been attributed to cortex, rectification might occur in retina, prior to the ganglion cell. Here we show that the Y ganglion cell does indeed respond to spatiotemporal contrast modulations of a second-order motion stimulus. Responses in an OFF ganglion cell are caused by an EPSP/IPSP sequence evoked from within the dendritic field; in ON cells inhibition is indirect. Inhibitory effects, which are blocked by tetrodotoxin, clamp the response near resting potential thus preventing saturation. Apparently the computation for second-order motion can be initiated by Y cells and completed by cortical cells that sum outputs of multiple Y cells in a directionally selective manner.

Introduction

The motion that we perceive when a coarse grating drifts across the retina is caused by spatiotemporal changes in luminance, a "first-order cue." But we also perceive motion when luminance is constant and only contrast changes over space and time. For example, when a fine grating is fixed on the retina, and its contrast is modulated by a coarse drifting "contrast envelope," we compute motion from spatiotemporal changes in contrast, a "second-order cue" (Figure 1) (Chubb and Sperling, 1988; Cavanaugh and Mather, 1989). First-order motion can be computed using an array of linear filters that sample the image over time at nearby points on the retina; the order of these outputs is determined to compute direction (Adelson and Bergen, 1985). But second-order motion requires an additional processing stage. The output of the array of linear filters must undergo some nonlinearity, such as rectification (i.e., responses cannot go negative), before it is used to compute direction (Chubb and Sperling, 1988; Cavanaugh and Mather, 1989; Baker, 1999).

Both stages for computing second-order motion were thought to occur in the visual cortex (Albright, 1992; Zhou and Baker, 1994; Mareschal and Baker, 1998, 1999). However, the rectification stage could in theory occur prior to the Y (α) retinal ganglion cell, found in all mammals, whose receptive field contains an array of rectifying subunits (Enroth-Cugell and Robson, 1966; Hochstein and Shapley, 1976; Peichl et al., 1987; Demb et al., 1999). Here we report that the Y cell does indeed respond to the fine-scale contrast modulations in a second-order motion stimulus. The response arises from an interaction between the rectifying synapse of a bipolar cell and the inhibitory synapse of a spiking amacrine cell. Thus, we propose a novel pathway for computing second-order motion that begins with rectification in the subunits of a Y cell; by combining the outputs of multiple Y cells, second-order motion could be computed directly by a direction-sensitive cell in cortex or tectum.

Results

Intracellular Recording of the Y Cell

We studied responses to cues for first- and second-order motion by recording intracellularly from the Y ("brisk-transient") ganglion cell in an in vitro preparation of the intact guinea pig retina (Cleland et al., 1971; Hochstein and Shapley, 1976; Demb et al., 1999, 2001). These cells were selected as the largest somas (20–25 μm diameter) comprising about 3%–5% of the cell bodies in the ganglion cell layer (Peichl et al., 1987). Responses to a spot of appropriate contrast (dim for an OFF cell, bright for an ON cell) were transient with peak responses $<$100 ms after the step change in contrast. All cells showed a center-surround organization and a dominant, second harmonic in response to contrast reversal of a high spatial frequency grating (Hochstein and Shapley, 1976). The sample included 31 cells (8 ON-center and 23 OFF-center) with resting potential of -62 ± 1.3 mV (mean $\pm$ SEM) and spontaneous firing of 10 ± 2 spikes/s. Maximum responses were as large as a 31 mV depolarization from the resting potential with 325 spikes/s and averaged 13.8 ± 1.5 mV with 170 ± 18 spikes/s. Input resistance was 38 ± 4 MΩ (n = 11). Cells remained in excellent condition with stable responses up to 2 hr.

The Y cell receptive field comprises two overlapping components: the standard center-surround and an array of narrow-field, nonlinear subunits (Hochstein and Shapley, 1976). Theoretically, the response to a second-order motion cue requires stimulation of only the nonlinear subunits. To determine a stimulus selective for the nonlinear subunits, we measured the spatial sensitivities of the center-surround and the subunits.

Spatial tuning was determined by measuring spike responses to gratings of different spatial frequency (Enroth-Cugell and Robson, 1966; Hochstein and Shapley, 1976). The first Fourier harmonic (F1) amplitude to a *drifting* grating was used to measure the spatial transfer function of the center-surround component, peaking at low frequencies and declining at high-frequencies (Figures 2A and 2B). The excitatory center was modeled with a broad Gaussian plus a narrow Gaussian to account for the sensitivity to frequencies $>$2 c/mm. This narrow Gaussian results in a spatial profile with a central "peak" (Figure 2D), consistent with the original description of cat Y cells recorded in vivo (Hochstein and Shapley, 1976). The inhibitory surround was modeled as a single

[1] Correspondence: demb@retina.anatomy.upenn.edu

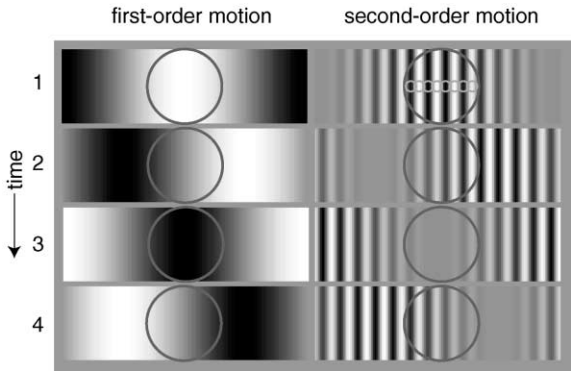

Figure 1. Cues for First- and Second-Order Motion

Stimulus frames are shown at four points in time. First-order motion stimulus is a sine-wave grating (1 cycle) drifting rightward. At the spatial scale of a cell's receptive field (circle), there is modulation of luminance (maximal at time 1, minimal at time 3). Second-order motion stimulus is a sine-wave "contrast envelope" (1 cycle) drifting rightward to reveal the underlying high spatial frequency carrier pattern (15 cycles). At the spatial scale of a cell's overall receptive field (large circle), there is no space-averaged modulation of luminance, but there is a strong modulation of contrast (maximal at time 1, minimal at time 3). Thus, the stimulus is "second-order" relative to the scale of the cell's receptive field. In order to detect the contrast modulations, the cell must combine the outputs of multiple subunits (small circles, one horizontal row shown at top) after the subunits undergo a nonlinearity.

broad Gaussian. The surround was relatively weak in most cells —its integral was only ~9% of the integral of the center (Figure 2B), but it was needed to achieve a good fit.

The spatial transfer function of the subunit receptive field was measured using a *contrast-reversing* grating. Spikes were measured for stationary gratings of various spatial frequencies whose contrast was modulated at 2 Hz. The second harmonic (F2) amplitude at 4 Hz is generated by the subunits (Hochstein and Shapley, 1976). The response peaked at an intermediate spatial frequency (Figures 2A and 2B). In addition, the subunits were sensitive to higher spatial frequencies than the center-surround. The second-order motion stimulus was created by weighting the contrast of a high spatial frequency "carrier pattern" by a lower-frequency "contrast envelope" (Figure 2C). We used a high spatial frequency for the carrier that should be visible to the Y cell's subunits (Figure 2D). The subunit was approximately six to seven times more sensitive than the center-surround at the frequency range of the carrier (Figure 2B). Thus, the response to the second-order motion stimulus depends on the fine spatial resolution of the Y cell's subunit.

Responses to Cues for First- and Second-Order Motion

The first-order motion cue was a coarse drifting grating. At the spatial scale of the cell's receptive field, the grating modulated luminance (i.e., the receptive field was covered by a dark bar followed by a light bar). The second-order motion cue was a coarse, drifting envelope that modulated the contrast of a fine, stationary grating (the carrier pattern). At the spatial scale of the cell's receptive field, space-averaged luminance remained constant over time, and the envelope instead modulated contrast (i.e., the receptive field was covered by a high-contrast pattern followed by a 0% contrast pattern; see Figure 1). The first-order cue caused the cell to depolarize by ~5 mV and to spike (Figure 3A), and the second-order cue caused the cell to depolarize by ~2 mV and to spike (Figure 3B). However, to the first- and second-order cues, both the membrane potential and spike responses behaved differently.

The membrane response to the first-order cue was sinusoidal at the drift frequency (F1 amplitude) with a smaller response at twice the drift frequency (F2 amplitude). At 6 Hz, the F1 amplitude accounted for nearly all of the response variance ($r^2 = 94.9\% \pm 0.8\%$), and the F2 amplitude accounted for only $2.4\% \pm 0.3\%$ ($n = 26$). The membrane response to the second-order cue was more complex. At 6 Hz, the F1 amplitude accounted for only half of the variance ($56.4\% \pm 5.1\%$), and the F2 amplitude accounted for $29.9\% \pm 4.5\%$ ($n = 26$). Because the sum of F1 and F2 amplitudes accounted for most of the response variance, we used them to quantify responses to both motion cues. For both cues the spike rate followed the membrane potential except that, due to the spike threshold that resulted from low maintained discharge, the response was strongly rectified (did not go negative).

Theoretically, the rectification caused by the ganglion cell's spike threshold cannot produce the response to the second-order motion cue. Instead, rectification must occur in the narrow-field subunits that drive the cell because these subunits are sensitive to the high spatial frequencies in the second-order stimulus (Baker, 1999). To demonstrate that rectification caused by the ganglion cell's spike threshold is not required, we injected positive current to raise the maintained discharge and thus reduce rectification. This *increased* the response to the second-order stimulus ($n = 3$; Figure 3C). A complementary result is found in area 17 simple cells. Area 17 cells sum linearly across space (i.e., no nonlinear subunits) and rectify only in their spike output, but they do not respond to second-order cues (Zhou and Baker, 1994). We conclude that rectification due to the ganglion cell's spike threshold is neither necessary nor sufficient to generate the response to the second-order motion cue.

We compared the shape of the temporal filter for first- and second-order motion cues by measuring responses to modulation at 1–12 Hz (Figure 3C). Responses were bandpass, peaking at an intermediate frequency (between 4 and 10 Hz; $n = 15$), and on average were the same for both cues (~7.5 Hz; Figure 3D). Responses of the membrane potential and spikes were similar except that at low temporal frequencies the spikes were relatively more attenuated (Lankheet et al., 1989). At all temporal frequencies, the second-order cue evoked a relatively large F2 component and was thus more biphasic. Thus, responses to first- and second-order cues showed similar bandpass temporal sensitivities but comprised distinct temporal profiles (i.e., distinct relative F1 and F2 amplitudes).

Control Experiments

Possibly, the response attributed to the second-order motion cue was actually caused by a first-order cue

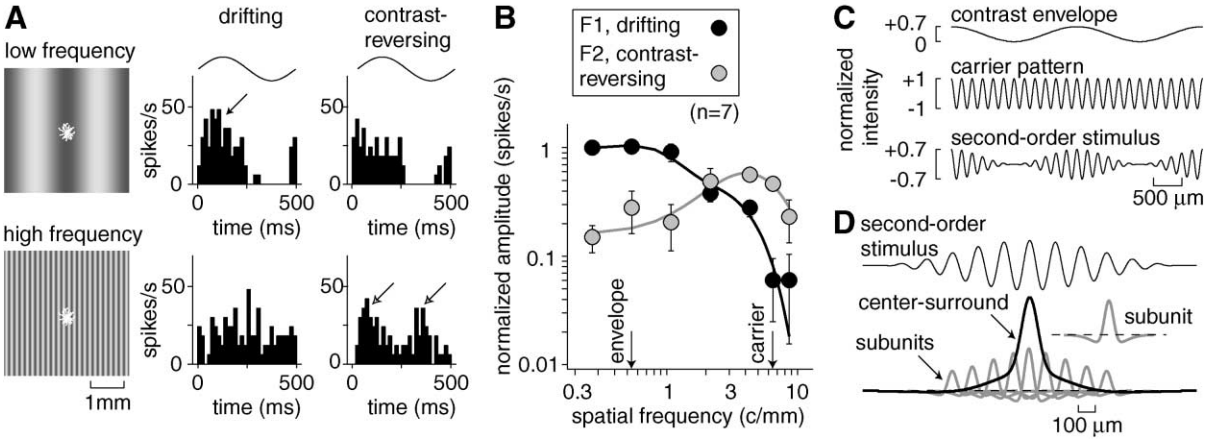

Figure 2. Design of the Stimulus for Second-Order Motion Contained Spatial Modulations on the Scale of the Y Cell's Subunit

(A) Standard protocol for measuring space constants of the center-surround receptive field and the nonlinear subunit. Center-surround responses, measured as the F1 amplitude to a drifting grating, were strong at low-frequency (arrow) but weaker at high-frequency. Subunit responses, measured as the F2 amplitude (frequency-doubled response) to a contrast-reversing grating, were relatively weak at low-frequency but strong at high-frequency (open arrows). Gratings were 40% contrast and drifted or reversed contrast at 2 Hz; bin size of post-stimulus time histogram (PSTH), 16.7 ms; typical dendritic field, 550 μm diameter.

(B) Average normalized response from seven cells (five OFF cells, two ON cells). In each cell, the F1 and F2 amplitudes (in spikes/s) were calculated by performing a Fourier transform on the spike PSTH and normalized by dividing all amplitudes by the F1 amplitude in response to the coarsest drifting grating, which was the maximal response (four out of seven cells) or the near-maximal response (three out of seven cells). Arrows mark the spatial frequencies of the "contrast envelope" and "carrier pattern" used in the second-order motion stimulus throughout the paper. At the carrier's high spatial frequency, the subunit response was approximately six to seven times more sensitive than the center-surround response.

(C) Second-order motion stimulus was a contrast envelope multiplied by a stationary carrier pattern. Drifting the envelope revealed the contrast in different regions of the stationary carrier.

(D) Center-surround and subunit profiles are derived from the responses in Figure B. (i.e., these profiles are the Fourier transforms of the fitted lines). Contrast modulations of the high-frequency carrier should optimally activate the Y cell's subunit. Gaussian space constants (full-width at half maximum or 2.35 SDs) are: center = 705 μm and 160 μm; surround = 1645 μm; subunit center = 89 μm; subunit surround = 282 μm. Subunit positions and amplitudes are approximate, but subunits most likely tile the retina and are most sensitive at the center of the receptive field (Hochstein and Shapley, 1976; Cohen and Sterling, 1992).

arising from a stimulus artifact (Zhou and Baker, 1994). Such an artifact could arise from insufficient linearization of the CRT display (gamma correction), so that the "mean luminance" is not actually half-way between the minimum and maximum luminance. If the display contained such a nonlinearity, the contrast envelope would actually modulate both contrast *and* luminance, and this would provide a first-order motion cue at the envelope's low spatial frequency (Zhou and Baker, 1996; Smith and Ledgeway, 1997). Similarly, if the display was perfectly linear, but the cone output contained a significant nonlinearity, this would provide a first-order motion cue at the envelope's low spatial frequency (MacLeod et al., 1992; Baker, 1999). We were partially reassured by the fact that responses to first- and second-order motion cues differed in their F1:F2 ratio, suggesting distinct temporal origins (Figures 3). Nevertheless, we performed three control experiments to address possible artifacts from the display.

First, we drifted a square-wave contrast envelope with discrete occluding bars at the calculated mean luminance of the carrier pattern (Figure 4A). If the average luminance of the dark and bright carrier bars differed significantly from the luminance of the occluding envelope, there would be a first-order motion cue (i.e., luminance modulation) at the low spatial frequency of the envelope. To correct for this putative luminance modulation, we added a luminance signal to the occluding envelope to shift it from dark (0) to bright (1.0) with small steps bracketing the calculated mean luminance (0.45, 0.48, 0.52, 0.55). If the standard envelope (0.50) caused a residual first-order motion cue, it would be nulled at one of these intermediate values. In fact, the response could not be nulled.

Second, we used an envelope that modulated the carrier pattern's temporal modulation instead of its contrast (Figure 4B). The temporal modulation was a counter-phase flicker of spatially localized regions of the carrier. The bars that were under the "flicker envelope" counterphased at 30 Hz, whereas bars in the adjacent region did not flicker at all (0 Hz). A region flickering at 30 Hz should resemble 0% contrast (mean luminance) because rapid flicker of dark and light carrier bars would temporally blur into gray, precisely matching the mean luminance of the stationary regions of the carrier (O'Keefe and Movshon, 1998). The responses to envelopes with flicker or contrast modulation, as in Figure 4A, were nearly identical (Figure 4B), suggesting that the calculated mean luminance based on the gamma correction was nearly perfect.

Finally, we defocused the microscope to attenuate high spatial frequencies (Figure 4C). This should not affect the response to the first-order motion cue by the coarse drifting grating and, in fact, did not. However, blurring the high-frequency carrier grating would reduce the modulation of contrast and thus reduce the re-

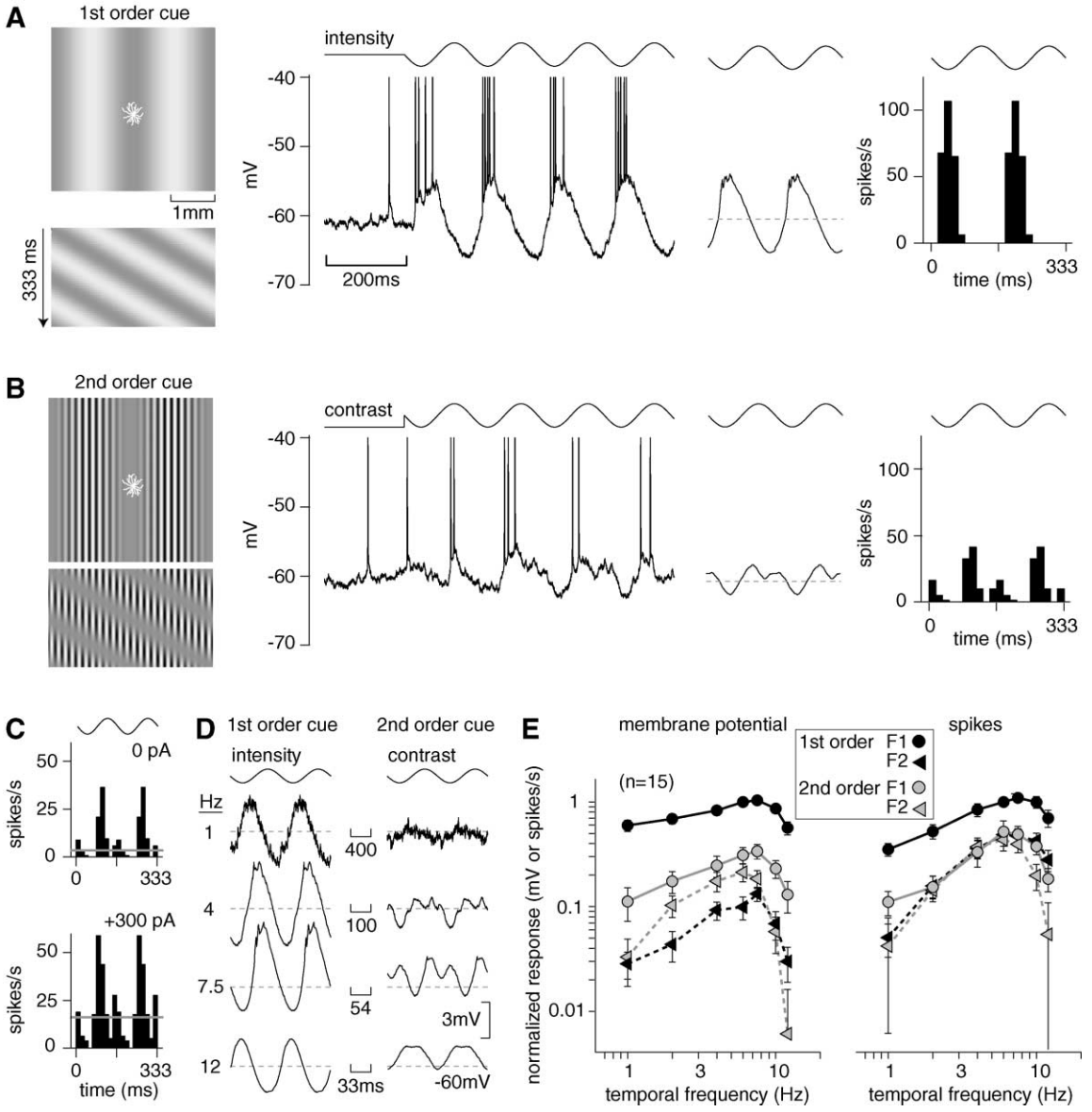

Figure 3. Retinal Ganglion Cell Responds to Both First- and Second-Order Motion Cues with Similar Temporal Sensitivities

(A) Coarse grating drifts rightward (6 Hz). Upper image shows spatial stimulus at one instant and lower image shows a space-time plot of two cycles. As each dark stripe drifts over the dendritic field, the OFF ganglion cell depolarizes and spikes. Average membrane potential (spikes clipped as in Demb et al. [1999]) and spike rate are shown, repeated for two cycles. In this and subsequent figures, unless noted otherwise, first-order motion cue is at 20% contrast and second-order motion cue is at 70% contrast; temporal frequency is 6 Hz; luminance grating and contrast envelope are sinusoidal with spatial frequency 0.54 cyc/mm; carrier pattern is sinusoidal with spatial frequency 6.5 cyc/mm; dashed line indicates resting potential.

(B) Coarse envelope drifts rightward (6 Hz) across a fine stationary grating (the "carrier"). Upper image shows spatial stimulus and lower image shows space-time plot. As the envelope drifts over the dendritic field, revealing the underlying carrier, the cell depolarizes and spikes.

(C) Spike response to second-order motion cue at 6 Hz without current (resting potential, −63 mV; maintained discharge, 3 spikes/s) and after injecting +300 pA (resting potential, −57 mV; maintained discharge, 16 spikes/s). Positive current reduced the ganglion cell's output (spike) rectification by increasing the discharge rate but increased the response to the second-order cue. Gray lines indicate maintained discharge during presentation of a blank screen at mean luminance.

(D) Ganglion cell responses (membrane potential) to motion at four temporal frequencies.

(E). Average response across cells normalized to response to first-order motion cue at 6 Hz (5 ON cells, 10 OFF cells). Fourier response amplitudes at the drift rate (F1) and twice the drift rate (F2) are shown for membrane potential and spikes. In this and subsequent figures, F1 and F2 amplitudes to a baseline stimulus (uniform screen at mean luminance) have been subtracted prior to averaging across cells; error bars represent ±SEM.

sponse, unless there was a residual low-frequency distortion product to act as a first-order motion cue (Zhou and Baker, 1994). In fact, blurring strongly reduced the response to the envelope ($p < 0.05$), and the response returned when the image was refocused (Figure 4C). Based on these three control experiments, we conclude

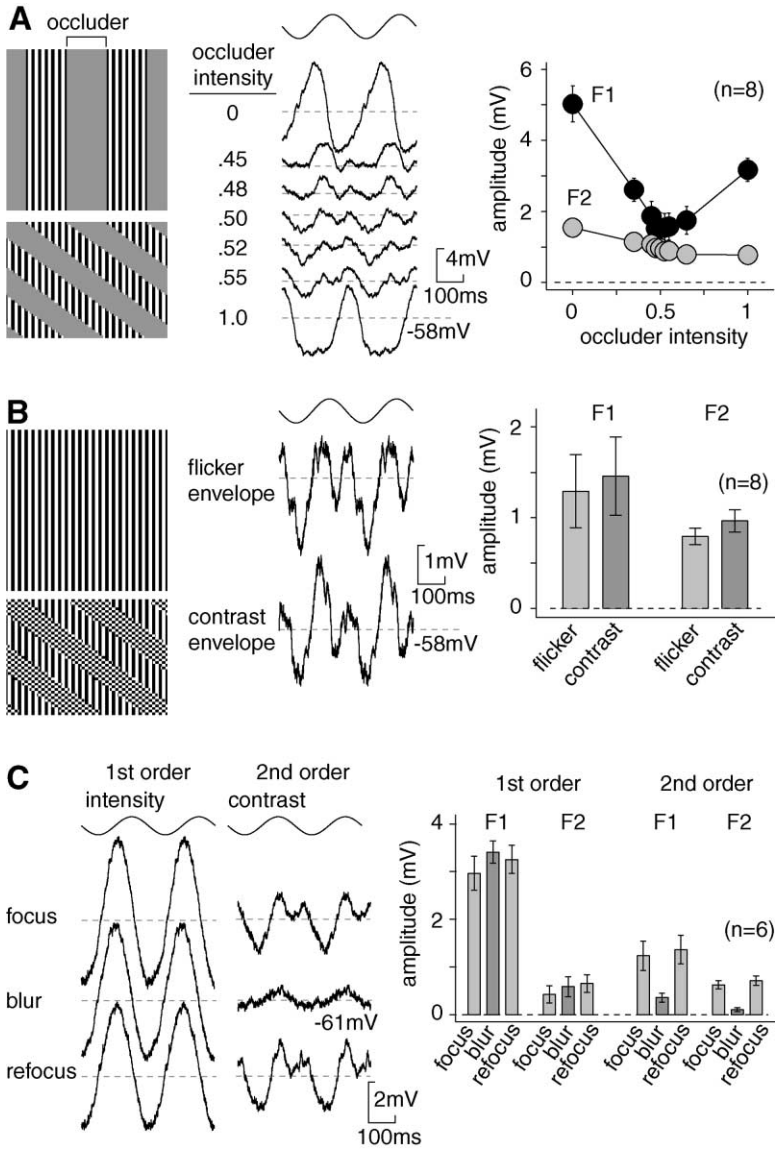

Figure 4. Three Control Experiments Verify that Response was Indeed to Second-Order Motion Cue

(A) Motion nulling. Drifting square-wave envelope had occluding stripes at the gamma-corrected mean luminance (0.50; see Results). In addition, a luminance signal was added or subtracted which made the occluding stripe vary from dark (0) to bright (1.0). Neither F1 nor F2 responses could be nulled as the intensity of the occluder was varied (two ON cells, six OFF cells). Carrier pattern was square-wave. All three control experiments were performed at a temporal frequency of 4 Hz; spatial frequencies were the same as Figure 3.

(B) Flicker-envelope. Envelope's occluder stripes were defined by 30 Hz flicker of the carrier bars or by contrast (same stimulus in [A]; in both cases envelopes and carriers were square-wave). F1 and F2 responses were nearly identical under the two conditions (two ON cells, six OFF cells).

(C) Image-blurring. Image was blurred by defocusing the microscope objective. Blurring did not decrease the response to the first-order cue but decreased significantly the response to the second-order cue (one ON cells, five OFF cells). Contrast envelope and carrier pattern were sinusoidal.

that drifting the envelope genuinely modulates contrast with minimal modulation of luminance. Consequently, the ganglion cell response to the modulation of contrast genuinely represents a response to second-order motion.

Cellular Mechanism

We next asked whether the circuits that drive the response to the second-order motion cue are local (cospatial with the ganglion cell's dendritic field) or global (over millimeters). To test this we presented stimuli to the full field or restricted it to the center or periphery (Figure 5A). The full-field and central stimuli evoked nearly identical responses. However, with the center masked, a peripheral stimulus evoked hardly any response. Thus, circuits for computing both first- and second-order motion are largely spanned by the ganglion cell's dendritic tree ($\sim$550 μm diameter) (Demb et al., 2001).

First- and second-order motion cues both modulate the ganglion cell's membrane potential rather symmetrically above and below the resting potential. If the hyperpolarizing component were caused by direct inhibition (opening a Cl^- or K^+ channel with E_{rev} negative to rest), injecting negative current should reduce it, and positive current should enhance it. This proved true for responses to both first- and second-order motion cues in OFF cells (n = 5; Figure 6). For ON cells, negative current *increased* hyperpolarizing responses to both motion cues (n = 2), suggesting that their hyperpolarizing components are caused by presynaptic inhibition of excitatory (bipolar cell) input. If the depolarizing component to motion cues were caused by direct excitation (opening a nonselective cation channel with E_{rev} = 0 mV), injecting negative current should enhance the response. This proved true for both ON and OFF cells, suggesting that their depolarizing components are caused by direct excitation from either ON or OFF bipolar cells.

Some of the $\sim$30 types of amacrine cells transmit signals via action potentials, and we considered whether

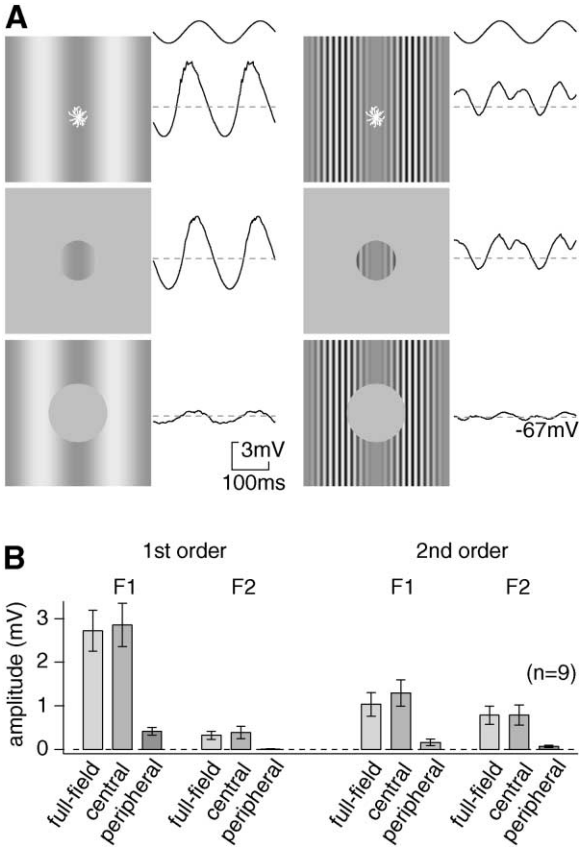

Figure 5. Responses to First- and Second-Order Motion Cues Arise Mostly from Circuits Cospatial with the Ganglion Cell's Dendritic Tree

(A) Response to first- and second-order motion cues with a full-field stimulus, a central stimulus (patch diameter = 1 mm), and a peripheral stimulus with a blank central mask (mask diameter = 1.5 mm).

(B) Average F1 and F2 amplitudes to first- and second-order motion cues in the three stimulus configurations (three ON cells, six OFF cells).

the pre- and postsynaptic inhibitory effects observed here are caused by spiking cells (Cook and Werblin, 1994; Stafford and Dacey, 1997; MacNeil and Masland, 1998). Blocking the ganglion cell's spikes intracellularly with QX-314 in the pipette did not affect responses either to first- or second-order motion cues (Figures 7A and 7B). But blocking amacrine cell spikes with TTX in the bath reduced the cell's hyperpolarizing response to the first-order motion cue and increased the depolarizing response. The response to the second-order motion cue was also altered; rather than modulating about the resting potential, there was a tonic depolarization of $\sim$4 mV which itself was modulated (Figure 7A). TTX affected the hyperpolarizing component in both OFF cells ($n = 7$) and ON cells ($n = 2$) (Figure 7B).

On average, TTX reduced the amplitude of the hyperpolarization (trough) and increased the amplitude of the depolarization (peak) (Figure 7C). This was most striking for the second-order cue where the initially hyperpolarizing trough shifted *positive* to the resting potential (Figure 7C, arrowheads). Thus, in response to the second-order cue, tonic inhibitory input from spiking amacrine cells normally balanced excitatory (bipolar cell) inputs, maintaining response modulations close to the resting potential.

TTX also reduced the biphasic structure of the response to the second-order motion cue. This biphasic pattern occurred during each stimulus cycle when the initial monophasic depolarization was interrupted by a hyperpolarization; TTX blocked the hyperpolarizing component (Figure 7). The F2 amplitude, which is sensitive to the biphasic response, was initially 0.93 $\pm$ 0.28 mV ($n = 9$) and decreased with TTX by 0.33 $\pm$ 0.14 mV ($p < 0.05$). In contrast, the F1 amplitude, a measure of the monophasic response, was initially 1.35 $\pm$ 0.42 mV and increased slightly with TTX by 0.07 $\pm$ 0.31 mV. Thus, the phasic inhibitory input during each cycle of second-order motion that creates the signature biphasic response must arise from a spiking amacrine cell.

Discussion

Ganglion Cells Contribute to the First Stage of Second-Order Motion Processing

To compute second-order motion, the general theory (developed for psychophysics and cortex) postulates an array of narrow spatial filters whose outputs are *rectified*; the order of these outputs is determined to *compute direction* (Baker, 1999; Chubb and Sperling, 1988; Graham et al., 1992; Wilson et al., 1992). We have shown that the Y retinal ganglion cell can accomplish the first stage of this computation because it integrates the output of multiple rectified subunits. The Y cell actually integrates two arrays of rectified subunits, one excitatory and one inhibitory (Figure 8A).

The excitatory array probably corresponds to transient bipolar cells (Euler and Masland, 2000; Demb et al., 2001), and the inhibitory array corresponds to spiking amacrine cells (Figure 8B) (Demb et al., 1999). Because an OFF ganglion cell's hyperpolarizing response to light "on" is caused by direct inhibition (Figure 6, top left), the amacrine cell that causes the inhibition is probably itself driven by the ON pathway (Figure 8B) (Roska and Werblin, 2001). This inhibition is distinct from the classical surround mechanism because it is sensitive to high spatial frequencies. Thus, it is probably driven by an amacrine cell with a narrow dendritic field. The narrow-field bipolar and amacrine subunits create a spatial sensitivity to the carrier that extends to the acuity limit of the animal (Zhou and Baker, 1996).

Mechanisms for Rectification

The rectification that drives the response to second-order motion could originate either within the bipolar and amacrine cells or possibly at the output of the cones that provide their excitatory drive. It was determined using psychophysical methods that cones probably contain an output rectification (compressive nonlinearity) that is especially prominent at high-contrast (He and MacLeod, 1998). For several reasons we believe that, for the second-order motion response measured here, this rectification in the cone output would not contribute significantly. First, cone output rectification is strongest at high temporal frequencies (>8 Hz) (He and MacLeod,

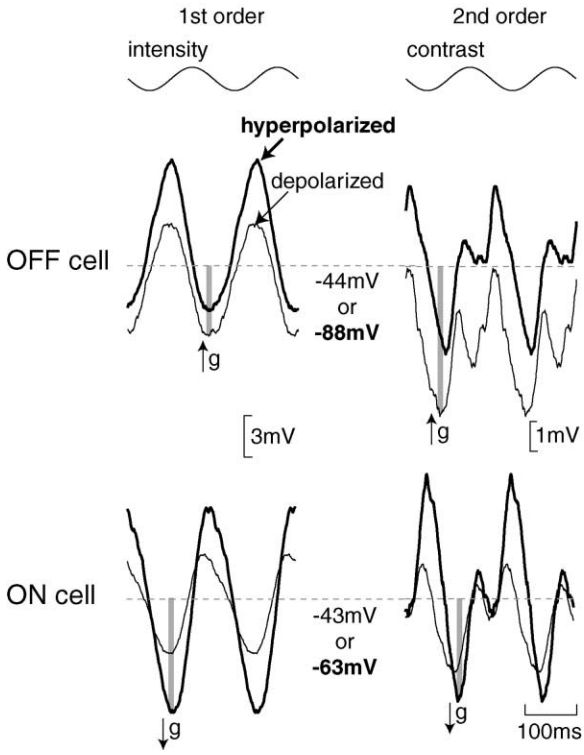

Figure 6. First- and Second-Order Motion Cues Cause Postsynaptic Inhibition in OFF Cells and Presynaptic Inhibition in ON Cells

Responses were measured to motion while cell was injected with depolarizing or hyperpolarizing current (±400 pA for OFF cell; ±500 pA for ON cell). Responses are shown relative to the resting membrane potential (dashed line) after injecting current. OFF cell's hyperpolarizing response to both motion cues (gray stripe) *increased* when the cell was depolarized, indicating an increase in conductance (g) and thus mostly postsynaptic inhibition. ON cell's hyperpolarizing response to both motion cues (gray stripe) *decreased* when the cell was depolarized indicating a decrease in conductance and thus mostly presynaptic inhibition of excitatory (bipolar cell) input. For both cells, depolarizing responses to motion cues decreased when the cell was depolarized, indicating an increase in conductance and thus mostly direct excitation, presumably from either ON or OFF bipolar cells. For both cells, the response without current (not shown) was intermediate to the responses with current. QX-314 (50 mM) was included in the pipette to block sodium channels; this avoided high-spike rates at depolarized potentials.

1998; Scott-Samuel and Georgeson, 1999), and yet we measured robust responses to second-order cues at low temporal frequencies (1–4 Hz) (Figures 3 and 4). Second, cone output rectification is negligible at low contrast (<40%) (He and MacLeod, 1998), and yet we were able to measure responses to second-order cues at 18% contrast (n = 3; data not shown). Finally, a cone output rectification predicts that all cells would respond to second-order motion (since all cells are ultimately driven by cones under photopic conditions), and this is

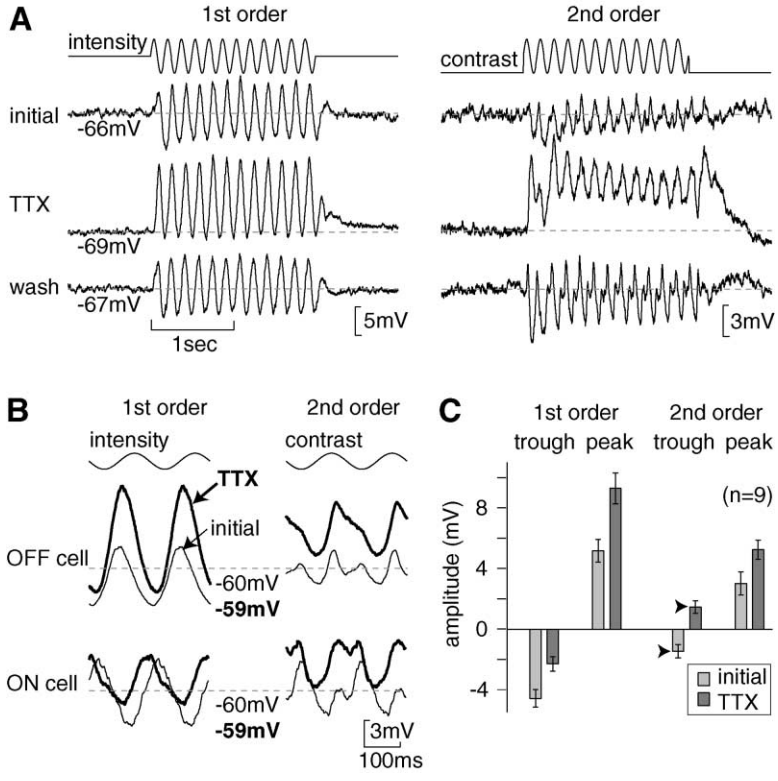

Figure 7. TTX Reduces the Hyperpolarizing Component of the Response

(A) Response to first- and second-order motion cues (OFF cell). TTX (200 nM) increased the depolarizing component and eliminated the hyperpolarizing component of responses to both first- and second-order motion cues. TTX also reduced the biphasic nature of the response to the second-order cue. QX-314 (50 mM) was included in the pipette to block ganglion cell's sodium channels; thus, the effect of TTX was on spiking amacrine cells.

(B) Averaged response of another OFF cell and an ON cell. QX-314 was included in the pipette. TTX markedly reduced the hyperpolarizing components for both cells and reduced the biphasic nature of the response to the second-order cue.

(C) The peak hyperpolarization (trough) and depolarization (peak), relative to the resting potential, are shown for motion responses (two ON cells, seven OFF cells). For the second-order cue, the initally hyperpolarizing trough shifted *positive* to the resting potential (arrowheads). For six of the nine cells QX-314 was included in the pipette.

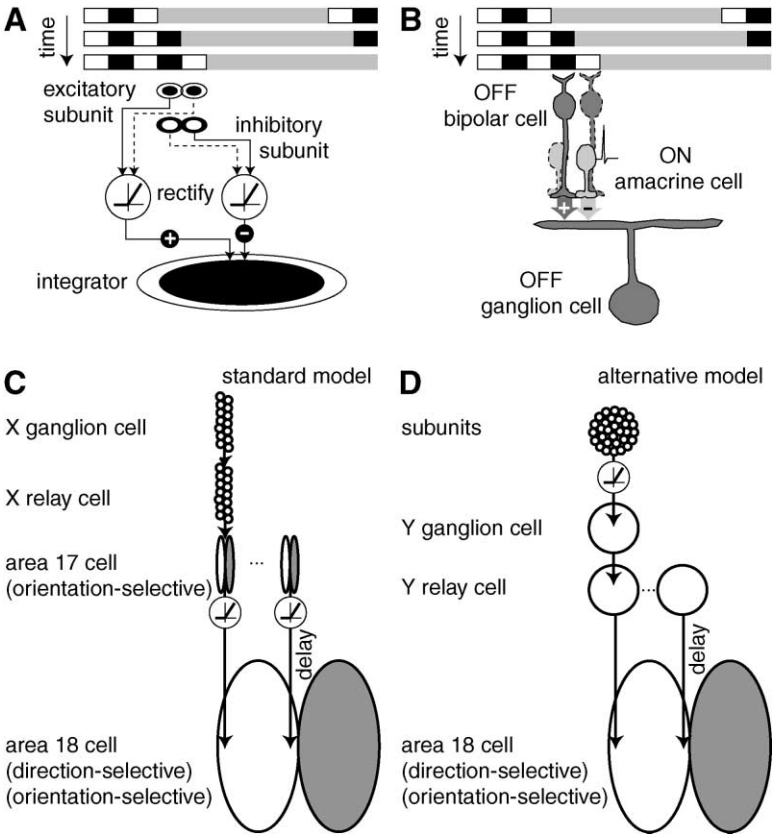

Figure 8. Circuits for Computing Second-Order Motion

(A) Conceptual model to explain an OFF ganglion cell's response to second-order motion cues. Stimulus shows a contrast envelope (gray region at mean luminance) drifting rightward to reveal the underlying carrier pattern (high-contrast) at the edge of the receptive field. Revealing the carrier pattern excites both an excitatory, OFF-center subunit, and an inhibitory, ON-center subunit. Subunit responses are rectified, so outputs can only increase and are integrated into a larger pool. Center-surround organization of the subunits and the integrator (i.e., OFF-center, ON-surround or vice versa) represent the typical center-surround organization of most retinal neurons.

(B) Circuit model. The excitatory subunit in (A) corresponds to an OFF-center bipolar cell. The inhibitory subunit corresponds to a spiking amacrine cell. Because an OFF cell's hyperpolarizing response to light "on" is caused by direct inhibition (Figure 6, top-left), this amacrine cell input is probably driven by the ON pathway. Amacrine inhibition would include both tonic and phasic components; blocking this inhibition would thus cause a tonic depolarization and a loss of the biphasic nature of the response to each stimulus cycle (Figure 7). Rectification at the output of bipolar and amacrine cells could be due to a combination of their transient response properties and low sustained release of neurotransmitter, such that their outputs can increase but not decrease. These rectified responses combine at the ganglion cell. Model for an ON ganglion cell would be similar except that inhibition would feed back on to the bipolar terminal rather than forward on to the ganglion cell (Figure 6).

(C) Standard model for processing second-order motion (Mareschal and Baker, 1998; 1999). Contrast modulations at high spatial frequency are detected by narrow-field linear X ganglion cells (receptive field centers indicated by circles). The orientation specificity of an area 17 cell arises because it sums inputs from neighboring X relay cells whose receptive fields fall in a line and because rows of inputs are either excitatory (white) or inhibitory (gray). Outputs of area 17 cells are rectified and combined by an area 18 cell. Orientation specificity of an area 18 cell arises because of elongated excitatory and inhibitory subregions. Direction selectivity arises because some synaptic inputs are delayed relative to others; activating the delayed input just prior to the nondelayed inputs would result in a larger temporal summation of excitatory inputs. Two stages of orientation selectivity allow separate orientation tuning to the carrier and the envelope (Mareschal and Baker, 1998; 1999).

(D) Alternative model for processing second-order motion. Contrast modulations at high spatial frequency are detected by the narrow-field nonlinear subunits whose outputs are rectified and combined by the Y cell. The outputs of multiple Y cells are relayed to area 18 where they are integrated by a direction-selective cell. A single stage of orientation selectivity, caused by elongated excitatory and inhibitory subregions of the area 18 cell, would result in strong orientation tuning for a low-frequency contrast envelope. Orientation tuning for a high-frequency carrier pattern could be driven by the orientation tuning of Y receptive fields (not shown here as oriented) which are similar among cells in a given region of retina (Levick and Thibos, 1980; Leventhal and Schall, 1983; Thibos and Levick, 1985; Soodak et al., 1987). Circles indicate the extent of the excitatory center of the subunit or the overall Y cell receptive field (see Figure 2).

clearly not the case for many cortical neurons tested under stimulus conditions similar to ours (Zhou and Baker, 1994). Thus, we conclude that the output rectification that is critical for the second-order response originates in the bipolar and amacrine cells presynaptic to the Y cell.

Several factors contribute to rectification at bipolar and amacrine outputs. Low basal rate of neurotransmitter release can increase more than it can decrease, causing mild rectification (Freed, 2000; Demb et al., 2001). In addition, the transient light response of certain types of bipolar and amacrine cells can create stronger rectification (Stafford and Dacey, 1997; Burkhardt and Fahey, 1998; Euler and Masland, 2000). The transient responses in turn arise from specific types of glutamate receptors on the dendritic tree (DeVries, 2000), inhibitory feedback onto the axon terminal (Dong and Werblin, 1998), and, in the case of amacrine cells, spiking in the axon terminal (Cook and Werblin, 1994; Stafford and Dacey, 1997).

The same retinal circuit would also drive responses to a first-order cue, such as a coarse drifting grating. In that case, the entire bipolar array would be stimulated simultaneously (e.g., for an OFF cell, by the dark bar) and then the amacrine array would be stimulated simultaneously (by the light bar). The Y cell's responses to first- and second-order cues could then be employed at a later stage to compute the direction of either first- or

second-order motion. This stage must integrate inputs from many Y cells, assessing their temporal order (Adelson and Bergen, 1985; Wolfe and Palmer, 1998).

Implications for Cortical Circuits and Behavior

The vertebrate retina conserves many features, one of which is a ganglion cell with properties like that of a mammalian Y/α cell. The circuit requires only broad summation of inputs from rectifying (transient) bipolar and amacrine cells. The characteristic α morphology has been identified in 20 mammalian species, including primate (Peichl et al., 1987). The characteristic Y physiology has been identified in goldfish (Bilotta and Abramov, 1989), cat (Enroth-Cugell and Robson, 1966; Hochstein and Shapley, 1976), rabbit (Caldwell and Daw, 1978), mouse (Stone and Pinto, 1993), guinea pig (Demb et al., 1999), and monkey (de Monasterio, 1978). In all cases, Y cells exhibit a frequency-doubled response to a high spatial frequency grating, the signature of the nonlinear subunits (Figure 2).

The second stage of second-order motion processing also appears to be broadly conserved across vertebrates. For example, the optomoter behavior of zebrafish can be driven by a second-order motion stimulus (Orger et al., 2000). This might be mediated by direction-sensitive cells in the optic tectum that integrate the output of multiple Y-like cells (Sajovic and Levinthal, 1982).

In cat, cells responding to second-order motion cues are rare in area 17 but common in area 18 where responses are driven strongly by Y ganglion cells (Ferster, 1990a, 1990b; Ferster and Jagadeesh, 1991; Zhou and Baker, 1994, 1996). Receptive fields in area 18 include a nondirection selective subunit similar to the Y cell's subunit (Zhou and Baker, 1996). Some area 18 cells are also relatively *insensitive* to the carrier's orientation (Mareschal and Baker, 1998, 1999) suggesting that the first stage rectification occurs in a subunit with a nearly concentric receptive field and only weak orientation tuning; cat Y cells indeed show such weak orientation tuning due to slightly oriented dendritic trees (Levick and Thibos, 1980; Leventhal and Schall, 1983; Thibos and Levick, 1985; Soodak et al., 1987). Thus, one possible pathway for computing second-order motion would involve directly reading out the responses of multiple Y cells (Figure 8D). However, other area 18 cells were *highly selective* for the carrier's orientation, and this selectivity was independent of the selectivity for the envelope's orientation (Mareschal and Baker, 1998, 1999). Thus, a second pathway might be postulated in which the rectification does not occur until after strong orientation-selectivity is established in a cortical cell (Figure 8C).

In monkey, Y-like cells project to the magnocellular layers of the LGN (Kaplan and Shapley, 1982; Marrocco et al., 1982), and thus they probably drive the V1 cells (Figure 4B, layer) that in turn drive direction-sensitive cells in area MT (Movshon and Newsome, 1996; Yabuta and Callaway, 1998). This may explain why MT cells respond to second-order motion cues (Albright, 1992; O'Keefe and Movshon, 1998; Smith et al., 1998). Another second-order cue for motion, defined by color (Dougherty et al., 1999), is also extracted in the retina by the blue-yellow ganglion cell (Dacey and Lee, 1994; Calkins et al., 1998; Chilchilnisky and Baylor, 1999) and used to compute the directional signal in MT (Seidemann et al., 1999; Wandell et al., 1999). These two examples may represent a general strategy for motion processing: the retina extracts second order features (i.e., contrast, color) and sends these signals to motion-sensitive areas of cortex where direction and speed are computed.

Cells were invariably less sensitive to second-order than to first-order motion cues (Figure 3D). This may explain why cortical cells (Albright, 1992; Zhou and Baker, 1994, 1996; O'Keefe and Movshon, 1998) and human and fish vision are also less sensitive to second-order cues (Smith and Ledgeway, 1997; Orger et al., 2000). Does this mean that second-order cues are unimportant? In a natural scene, second-order motion cues are correlated with first-order motion cues (Baker, 1999). So, sensitivity to second-order (i.e., computed) features, such as contrast or color, must enhance overall sensitivity to motion. In addition, second-order signals remove the contrast-dependence of perceived speed (Blakemore and Snowden, 2000). Certainly, all features that enhance sensitivity to local motion will improve detection of prey and predator and offer a selective advantage.

Experimental Procedures

Intracellular Recording

From a guinea pig anesthetized with ketamine (1.0 cc kg^{-1}), xylazine (1.0 cc kg^{-1}), and pentobarbital (3.0 cc kg^{-1}), an eye was removed following which the animal was killed by anesthetic overdose. These procedures were performed in accordance with University of Pennsylvania and National Institutes of Health guidelines. The whole retina, including the pigment epithelium, choroid, and sclera, was mounted flat in a chamber on a microscope stage. Retina was superfused ($\sim$4 ml/min) with oxygenated (95% O, 5% CO_2) Ames medium (Sigma, St. Louis, MO) at 33°C $\pm$ 1°C. Acridine orange (0.001%, Molecular Probes, Eugene, OR) added to the superfusate allowed ganglion cell somas to be identified by fluorescence during brief exposure to near UV light. Large somas (20–25 μm) in the visual streak (dorsal retina, within 4 mm of the optic disk) were targeted for intracellular recording.

Glass electrodes (tip resistance 80–200 MΩ) contained 1% pyranine (Molecular Probes) and 2% Neurobiotin (Vector Laboratories, Burlingame, CA) in 2 M potassium acetate. In some experiments, lidocaine N-ethyl bromide (QX-314, Research Biochemicals, Natick, MA) was added to the pipette solution. QX-314 blocks sodium channels in the recorded ganglion cell. This was used to test the specific effects of TTX on amacrine cell spikes and when injecting currents into the cell. The injected current probably affected the soma more than the dendrites; however, there must have been an effect at the dendrites since injected current strongly influenced the response amplitude (Figure 6), and the synapses are primarily on the dendrites (Stevens et al., 1980). To be conservative, we did not estimate reversal potentials but only examined the direction of the effect to injected current.

Membrane potential was amplified (NeuroData, IR-283, NeuroData Instruments Corp., Delaware Water Gap, PA), continuously sampled at 5 kHz, and stored on computer (AxoScope software, Axon Instruments, Foster City, CA). Data were analyzed with programs written in Matlab (Mathworks, Natick, MA). Spikes were detected off-line and removed computationally to allow analysis of membrane potential (Demb et al., 1999). Tetrodotoxin (TTX, Sigma, St. Louis, MO) added to the superfusate terminated spiking in $\sim$10 s, leaving just the graded response. Responses were averaged over 2–20 s of visual stimulation. Resting potential was determined by averaging the membrane potential over 1 s before and after each stimulus.

Visual Stimulus

The stimulus was displayed on a miniature monochrome computer monitor (Lucivid MR1-103, Microbrightfield, Colchester, VT) projected through the top port of the microscope through a 2.5× objective and focused on the photoreceptors. Mean luminance of the green phosphor corresponded to $\sim 10^5$ isomerizations cone^{-1} s^{-1}. Monitor resolution was 852 × 480 pixels with 60 Hz vertical refresh; stimuli were confined to a square with 430 pixels to a side (3.7 mm on the retina). A typical receptive field center was ~75 pixels in diameter. The relationship between gun voltage and monitor intensity was linearized in software with a lookup table. Stimuli were defined by percent Michelson contrast: $100 \times (I_{max} - I_{min})/(I_{max} + I_{min})$, where I_{max} and I_{min} are the peak and trough intensities. The contrast of fine gratings was corrected based on a measured optical line spread of 40 μm (full-width at half-height) (Demb et al., 1999). Stimuli were programmed in Matlab using extensions provided by the high-level Psychophysics Toolbox (Brainard, 1997) and the low-level Video Toolbox (Pelli, 1997).

Acknowledgments

This work was supported by National Eye Institute grants F32-EY06850 (JBD), T32-EY07035 (KZ), and RO1-EY00828 (PS). We thank Dr. Ben Backus and three anonymous reviewers for their helpful comments on the manuscript. We thank Sharron Fina for help in preparing the manuscript.

Received May 14, 2001; revised September 7, 2001.

References

Adelson, E.H., and Bergen, J.R. (1985). Spatiotemporal energy models for the perception of motion. J. Opt. Soc. Am. *2*, 284–299.

Albright, T.D. (1992). Form-cue invariant motion processing in primate visual cortex. Science *255*, 1141–1143.

Baker, C.L. (1999). Central neural mechanisms for detecting second-order motion. Curr. Opin. Neurobiol. *9*, 461–466.

Bilotta, J., and Abramov, I. (1989). Orientation and direction tuning of goldfish ganglion cells. Vis. Neurosci. *2*, 3–13.

Blakemore, M.R., and Snowden, R.J. (2000). Textured backgrounds alter perceived speed. Vision Res. *40*, 629–638.

Brainard, D.H. (1997). The psychophysics toolbox. Spat. Vis. *10*, 433–436.

Burkhardt, D.A., and Fahey, P.K. (1998). Contrast enhancement and distributed encoding by bipolar cells in the retina. J. Neurophysiol. *80*, 1070–1081.

Cavanaugh, P., and Mather, G. (1989). Motion, the long and short of it. Spat. Vis. *4*, 103–129.

Caldwell, J.H., and Daw, N.W. (1978). New properties of rabbit retinal ganglion cells. J. Physiol. *276*, 257–276.

Calkins, D.J., Tsukamoto, Y., and Sterling, P. (1998). Microcircuitry and mosaic of a blue-yellow ganglion cell in the primate retina. J. Neurosci. *18*, 3373–3385.

Chilchilnisky, E.J., and Baylor, D.A. (1999). Receptive-field microstructure of blue-yellow ganglion cells in primate retina. Nat. Neurosci. *2*, 889–893.

Chubb, C., and Sperling, G. (1988). Drift-balanced random stimuli, a general basis for studying non-Fourier motion perception J. Opt. Soc. Am. A. *5*, 1986–2007.

Cleland, B.G., Dubin, M.W., and Levick, W.R. (1971). Sustained and transient neurones in the cat's retina and lateral geniculate nucleus. J. Physiol. *217*, 473–496.

Cohen, E., and Sterling, P. (1992). Parallel circuits from cones to the on-beta ganglion cell. Eur. J. Neurosci. *4*, 506–520.

Cook, P.B., and Werblin, F.S. (1994). Spike initiation and propagation in wide field transient amacrine cells of the salamander retina. J. Neurosci. *14*, 3852–3861.

Dacey, D.M., and Lee, B.B. (1994). The 'blue-on' opponent pathway in primate retina originates from a distinct bistratified ganglion cell type. Nature *367*, 731–735.

Demb, J.B., Haarsma, L., Freed, M.A., and Sterling, P. (1999). Functional circuitry of the retinal ganglion cell's nonlinear receptive field. J. Neurosci. *19*, 9756–9767.

Demb, J.B., Zaghloul, K., Haarsma, L., and Sterling, P. (2001). Bipolar cells contribute to nonlinear spatial summation in the brisk-transient (Y) ganglion cell in mammalian retina. J. Neurosci. *21*, 7447-7454.

de Monasterio, F.M. (1978). Properties of concentrically organized X and Y ganglion cells of macaque retina. J. Neurophysiol. *41*, 1394–1417.

DeVries, S.H. (2000). Bipolar cells use kainate and AMPA receptors to filter visual information into separate channels. Neuron *28*, 847–856.

Dong, C.-J., and Werblin, F.S. (1998). Temporal contrast enhancement via $GABA_C$ feedback at bipolar terminals in the tiger salamander retina. J. Neurophysiol. *79*, 2171–2180.

Dougherty, R.F., Press, W.A., and Wandell, B.A. (1999). Perceived speed of colored stimuli. Neuron *24*, 893–899.

Enroth-Cugell, C., and Robson, J.G. (1966). The contrast sensitivity of retinal ganglion cells of the cat. J. Physiol. *187*, 517–552.

Euler, T., and Masland, R.H. (2000). Light-evoked responses of bipolar cells in a mammalian retina. J. Neurophysiol. *83*, 1817–1829.

Ferster, D. (1990a). X- and Y-mediated synaptic potentials in neurons of areas 17 and 18 of cat visual cortex. Vis. Neurosci. *4*, 115–133.

Ferster, D. (1990b). X- and Y-mediated current sources in areas 17 and 18 of cat visual cortex. Vis. Neurosci. *4*, 135–145.

Ferster, D., and Jagadeesh, B. (1991). Nonlinearity of spatial summation in simple cells of areas 17 and 18 of cat visual cortex. J. Neurophysiol. *66*, 1667–1679.

Freed, M.A. (2000). Rate of quantal excitation to a retinal ganglion cell evoked by sensory input. J. Neurophysiol. *83*, 2956–2966.

Graham, N., Beck, J., and Sutter, A. (1992). Nonlinear process in spatial-frequency channel models of perceived texture segregration, effects of sign and amount of contrast. Vision Res. *32*, 719–743.

He, S., and MacLeod, D.I.A. (1998). Contrast-modulation flicker: dynamics and spatial resolution of the light adaptation process. Vision Res. *38*, 985–1000.

Hochstein, S., and Shapley, R.M. (1976). Linear and nonlinear spatial subunits in Y cat retinal ganglion cells. J. Physiol. *262*, 265–284.

Kaplan, E., and Shapley, R.M. (1982). X and Y cells in the lateral geniculate nucleus of macaque monkeys. J. Physiol. *330*, 125–143.

Lankheet, M.J., Molenaar, J., and van de Grind, W.A. (1989). The spike generating mechanism of cat retinal ganglion cells. Vision Res. *29*, 505–517.

Leventhal, A.G., and Schall, J.D. (1983). Structural basis of orientation sensitivity of cat retinal ganglion cells. J. Comp. Neurol. *220*, 465-475.

Levick, W.R., and Thibos, L.N. (1980). Orientation bias of cat retinal ganglion cells. Nature *286*, 389-390.

MacLeod, D.I.A., Williams, D.R., and Makous, W. (1992). A visual nonlinearity fed by single cones. Vision Res. *32*, 347–363.

MacNeil, M.A., and Masland, R.H. (1998). Extreme diversity among amacrine cells, implications for function. Neuron *20*, 971–982.

Mareschal, I., and Baker, C.L. (1998). A cortical locus for the processing of contrast-defined contours. Nat. Neurosci. *1*, 150–154.

Mareschal, I., and Baker, C.L. (1999). Cortical processing of second-order motion. Vis. Neurosci. *16*, 527–540.

Marrocco, R.T., McClurkin, J.W., and Young, R.A. (1982). Spatial summation and conduction latency classification of cells of the lateral geniculate nucleus of macaques. J. Neurosci. *2*, 1275–1291.

Movshon, J.A., and Newsome, W.T. (1996). Visual response properties of striate cortical neurons projecting to area MT in macaque monkeys. J. Neurosci. *16*, 7733–7741.

O'Keefe, L.P., and Movshon, J.A. (1998). Processing of first- and second-order motion signals by neurons in area MT of the macaque monkey. Vis. Neurosci. *15*, 305–317.

Orger, M.B., Smear, M.C., Anstis, S.M., and Baier, H. (2000). Percep-

tion of Fourier and non-Fourier motion by larval zebrafish. Nat. Neurosci. *3*, 1128–1133.

Peichl, L., Ott, H., and Boycott, B.B. (1987). Alpha ganglion cells in mammalian retinae. Proc. R. Soc. Lond. B Biol. Sci. *231*, 169–197.

Pelli, D.G. (1997). The VideoToolbox software for visual psychophysics, transforming numbers into movies. Spat. Vis. *10*, 437–442.

Roska, B., and Werblin, F. (2001). Vertical interactions across ten parallel, stacked representations in the mammalian retina. Nature *410*, 583–587.

Sajovic, P., and Levinthal, C. (1982). Visual response properties of zebrafish tectal cells. Neuroscience *7*, 2427–2440.

Scott-Samuel, N.E., and Georgeson, M.A. (1999). Does early nonlinearity account for second-order motion? Vision Res. *39*, 2853–2865.

Seidemann, E., Poirson, A.B., Wandell, B.A., and Newsome, W.T. (1999). Color signals in area MT of the macaque monkey. Neuron *24*, 911–917.

Smith, A.T., and Ledgeway, T. (1997). Separate detection of moving luminance and contrast modulations, fact or artifact? Vision Res. *37*, 45–62.

Smith, A.T., Greenlee, M.W., Singh, K.D., Kraemer, F.M., and Hennig, J. (1998). The processing of first- and second-order motion in human visual cortex assessed by functional magnetic resonance imaging (fMRI). J. Neurosci. *18*, 3816–3830.

Soodak, R.E., Shapley, R.M., and Kaplan, E. (1987). Linear mechanism of orientation tuning in the retina and lateral geniculate nucleus of the cat. J. Neurophysiol. *58*, 267–275.

Stafford, D.K., and Dacey, D.M. (1997). Physiology of the A1 amacrine, a spiking, axon-bearing interneuron of the macaque monkey retina. Vis. Neurosci. *14*, 507–522.

Stevens, J.K., McGuire, B.A., and Sterling, P. (1980). Toward a functional architecture of the retina: serial reconstruction of adjacent ganglion cells. Science *207*, 317–319.

Stone, C., and Pinto, L.H. (1993) Response properties of ganglion cells in the isolated mouse retina. Vis. Neurosci. *10*, 31–39.

Thibos, L.N., and Levick, W.R. (1985). Orientation bias of brisk-transient y-cells of the cat retina for drifting and alternating gratings. Exp. Brain Res. *58*, 1–10.

Wandell, B.A., Poirson, A.B., Newsome, W.T., Baseler, H.A., Boynton, G.M., Huk, A., Gandhi, S., and Sharpe, L.T. (1999). Color signals in human motion-selective cortex. Neuron *24*, 901–909.

Wilson, H.R., Ferrera, V.P., and Yo, C. (1992). A psychophysically motivated model for two-dimensional motion perception. Vis. Neurosci. *9*, 79–97.

Wolfe, J., and Palmer, L.A. (1998). Temporal diversity in the lateral geniculate nucleus of cat. Vis. Neurosci. *15*, 653–675.

Yabuta, N.H., and Callaway, E.M. (1998). Functional streams and local connections of layer 4C neurons in primary visual cortex of the macaque monkey. J. Neurosci. *18*, 9489–9499.

Zhou, Y.X., and Baker, C.L. (1994). Envelope-responsive neurons in areas 17 and 18 of cat. J. Neurophysiol. *72*, 2134–2150.

Zhou, Y.X., and Baker, C.L. (1996). Spatial properties of envelope-responsive cells in area 17 and 18 neurons of the cat. J. Neurophysiol. *75*, 1038–1050.